Desalination and Water Treatment
www.deswater.com

doi: 10.5004/dwt.2019.24270

158 (2019) 140–151
August

Potential of Saudi natural clay as an effective adsorbent in heavy metals removal from wastewater

M.I. Khan[a,*], M.K. Almesfer[a], M. Danish[a], I.H. Ali[b], H. Shoukry[c], R. Patel[d], J. Gardy[e], A.S. Nizami[f], M. Rehan[f,*]

[a]*Department of Chemical Engineering, College of Engineering, King Khalid University, Abha, Saudi Arabia, email: mkaan@kku.edu.sa (M.I. Khan)*
[b]*Department of Chemistry, College of Science, King Khalid University, Abha, Saudi Arabia*
[c]*Housing and Building National Research Center (HBRC), Building Physics Institute (BPI), Cairo, Egypt*
[d]*Chemical Engineering Department, School of Engineering, University of Bradford, Bradford, UK*
[e]*School of Chemical and Process Engineering, University of Leeds, Leeds, LS2 9JT, UK*
[f]*Centre of Excellence in Environmental Studies (CEES), King Abdulaziz University, Jeddah, Saudi Arabia, email: mkaan@kku.edu.sa (M.I. Khan), dr.mohammad_rehan@yahoo.co.uk (M. Rehan)*

Received 26 April 2018; Accepted 13 April 2019

ABSTRACT

This study aims to examine the potential of natural clay mineral from the southern part of Saudi Arabia as an effective adsorbent material for the removal of heavy metal ions of cadmium (Cd) and nickel (Ni) from aqueous solutions. The SEM analysis showed that clay particles had mixed shapes such as elongated rod-like and rectangular shape having rough corners with larger particles of 2–8 μm in size and smaller particles in the sub-micron size range. X-ray diffraction data revealed that clay particles had a good crystalline structure and composed of a mixture of various minerals including feldspar, illite, quartz, calcite, and gypsum. The BET surface area was found to be 35 ± 1 m^2/g and the average pore size and pore volume of 6.5 ± 0.5 nm and 5.7e-02 cc/g, respectively. The X-ray fluorescence analysis of clay showed main compounds of SiO_2 (47.33%), Al_2O_3 (18.14%), Fe_2O_3 (15.89%) with many others such as CaO, MgO, TiO_2, and K_2O in minor quantities. It was found that 1.2 g of clay removed up to 99.5% of Ni and 97.5% of Cd from 40 ppm aqueous solutions. The metal removal efficiencies were increased from around 95% up to 99% by increasing the pH of aqueous solutions from 4 to 11. The adsorption of Ni and Cd ions on Saudi clay was relatively fast, and up to 97% of ions were removed from solution within 45 min. The SEM-EDX and BET analysis for recycled clays further confirmed that the metal ions were removed from water through adsorption onto the clay. The experimental data fitted well with Langmuir and Freundlich isotherms. The maximum adsorption capacity of clay for Cd and Ni from isotherms was found to be 3.3 and 2.7 mg/g respectively. The findings of this study confirm the potential role of Saudi natural clay in wastewater treatment processes as a cheap, environment-friendly and safe natural adsorbent material.

Keywords: Heavy metals; Natural clay; Adsorption; Wastewater; Water pollution

1. Introduction

Pollutants and contaminants in the form of heavy metals in water, soil and underground systems present significant health risks and environmental concerns [1]. The accumulation of heavy metals such as copper (Cu), chromium (Cr), cadmium (Cd), nickel (Ni), lead (Pb), and barium (Ba) in the human body leads to serious health issues including

* Corresponding authors.
mkaan@kku.edu.sa (M. I. Khan)
dr.mohammad_rehan@yahoo.co.uk (M. Rehan)

chronic diseases and disorders [2]. Among these, Cd, Ni, and Cu are more toxic to human and animal health if their concentration in water is exceeding the allowable limits [3]. In addition, the excessive amounts of heavy metals in wastewater limit the efficiencies of biological treatment methods. Moreover, heavy metals can infiltrate into the groundwater through aquifers [4]. In drinking water, the concentration of Ni and Cd should not exceed 0.015 and 0.01 mg/g, respectively [5]. Therefore, the removal of heavy metal contaminants from wastewater and drinking water is a challenge for today's engineers and scientists [6].

There are various water and wastewater treatment methods, including reverse osmosis, precipitation, flocculation and sedimentation, distillation and vaporization, solvent extraction, and filtration, used as conventional techniques for heavy metals removal [7–10]. The high cost associated with most of these methods is a limiting factor in their commercialization [11]. Adsorption has emerged as a promising solution for removing heavy metal ions in recent years, as being the simplest, economical and environment-friendly technique [7]. In addition, adsorption has become the most widely used method nowadays due to the ease of fabrication of equipment, installation and operation, and less associated costs [12,13].

An array of materials have been utilized as adsorbent materials to remove heavy metals from aqueous solutions [14–20]. For example, activated carbon as the adsorbent material has been used extensively for heavy metal removal [21–23]. Similarly, natural waste materials are used as adsorbent materials for heavy metal removals [24–26]. Moreover, different clay-based minerals have been used as adsorbent materials for the same purpose [27–29]. High isothermal adsorption efficiencies are reported for various clay materials in different parts of the world, including South Africa, Saudi Arabia, and the United States [4,30]. The metal removal efficiencies of clay are examined under various conditions including clay dosage, contact time, pH, and initial metal ions concentration.

There is a strong need to explore cheaper, natural, environment-friendly and efficient adsorbent materials, especially in the developing countries such as Saudi Arabia which is located in an arid region with limited water resources. As a result, the necessity of potable water is critical and even increasing with the growing population and living standards. Moreover, there are no natural rivers and lakes, and the underground water wells are not capable of meeting the current and projected gap between water demand and supply. On average 150 mm of rain occurs every year in the country [4]. Therefore, the need for wastewater treatment is crucial to meet the water supply in the agriculture and industrial sectors. The use of indigenous natural clay as adsorbent materials has been examined earlier for treating wastewater and removing heavy metals [4,30–33]. Clay minerals from different parts of the world have been studied for their potential role as absorbent materials to remove heavy metals from wastewater shown in Table 1. However, the reported use of natural clay as an adsorbent material from the Southern region of Saudi Arabia that is rich in clay minerals is scarce in the literature, which was the focus of this study.

This study aims to examine some naturally occurring clay minerals from the Southern part of Saudi Arabia as adsorbent materials for the removal of Cd and Ni from artificial wastewater. The effects of clay adsorbent dosage, pH, initial metals ion concentration and contact time were investigated and compared with other clay adsorbent materials for the removal of similar heavy metal ions.

2. Materials and methods

2.1. Collection and preparation of the clay adsorbents

The clay mineral used for this work was collected from the Southern region of Saudi and grounded into the powdered form using a mortar and pestle. The prepared clay powders were then sieved using a 125 mesh size sieve. The obtained clay powders were used without any further treatment.

Table 1
Heavy metal ions removal and recovery from aqueous solutions using various kinds of clay adsorbents

Metal ions type	Type of clay adsorbent	Reference
Cr and Pb	Iraqi MMT	[11]
Cu, Ni, Cd, Co, Zn and Pb	Bentonite and modified bentonite	[4,31–34,51]
Cu, Ni, Co, Mn and Cd	Kaolinite and metakaolinite	[35,37]
Cd and Pb	Calcite	[36,38]
Pb, Cu and Zn	Natural and activated clays	[30,39,40]
Cu, Cd and Pb	Geothilte	[41]
Ni	Silylated or organoclays	[42]
Th(IV)	Illite	[43]
Cd and Ni	Expanded perlite	[44]
Cu	Tunisian clay	[45]
Zn	Brazillian grey clay	[46]
Cr and Cd	Landfill clay	[47]
Cd	Smectite and lewatite	[54]
Pb, Cd and Ni	Kaolinite and MMT	[55]
Ni and As	Natural sepiolite	[56]

2.2. Batch adsorption experiments

With the ease of operation and the robust control of variables, adsorption experiments were performed in a batch process. In each experiment, 50 mL solutions containing 40 ppm concentration of the metal ions were placed into 50 mL conical flasks with 1 g clay and were mixed for 1 h. The contents were then filtered and the filtrate collected was analyzed by atomic absorption spectroscopy (AAS). The effects of other variables such as clay dosage, solution pH, contact time and initial concentration on adsorption efficiency were investigated. Removal efficiency in each case was calculated using Eq. (1):

$$\text{Removal efficiency}\left(\%\right)=\frac{\left(C_0-C_e\right)}{C_0}\times 100 \tag{1}$$

where C_0 is the initial concentration of the metal ions and C_e is the residual or equilibrium concentration at the end of each experiment. The adsorption capacity of the clay can be calculated using Eq. (2):

$$q_e=\frac{V}{m}\times\left(C_0-C_e\right) \tag{2}$$

where q_e is the removal capacity of the adsorbent (mg of metal/g of the clay), V is the volume of the prepared sample (liters), m is the mass of the adsorbent in grams, C_0 and C_e are the initial and final metal ions concentrations, respectively.

2.3. Analytical techniques

Stock solutions of Cd and Ni metal ions were prepared by dissolving appropriate amounts of cadmium chloride hydrate ($CdCl_2{\cdot}H_2O$, Sigma-Aldrich, US) and nickel(II) nitrate hexahydrate ($Ni(NO_3)_2{\cdot}6H_2O$, Sigma-Aldrich) in deionized water. Diluted hydrochloric acid and sodium hydroxide were used in preparing solutions of different pH. Stock solutions of 1,000 ppm of Ni metal ions were prepared by dissolving the appropriate quantity of $Ni(NO_3)_2{\cdot}6H_2O$ in deionized water. Appropriate quantities of stock solutions were diluted to obtain 40 ppm of the metal ions solutions. All the experiments were conducted with 40 ppm solutions except for the effect of initial metal ions concentration for which the concentration ranged from 10 to 60 ppm in steps of 10. The prepared solutions were poured into a series of 50 mL conical flasks and appropriate amounts of clay added to each. The mixture was then stirred for 2 h.

The contents were then immediately filtered, and the filtrate was analyzed using the AAS instrument (SpectrAA 220). AAS was used to measure the residue of heavy metal ions after treatment with the clay under various conditions. Standard solutions of 1, 3, 5, 7, 9, and 10 ppm were prepared for the calibration of the AAS instrument prior to the actual sample measurements. Standard solutions were prepared by dilution of the stock solutions. In each case, X amount of stock solution was pipetted into a volumetric flask (50 mL), and the dilutions were carried out according to the standard formula of $C_1V_1 = C_2V_2$, where C_1 is the concentration before dilution (stock solution), V_1 is volume before dilution, C_2 is desired concentration and V_2 is the desired volume. Once, the instrument was calibrated, and the standard graph was obtained, the actual measurements of the heavy metal ions residual determination were carried out. For the case of Ni, the selected wavelength was 232 nm, and the slit width was 0.2 nm while for Cd, the wavelength was 228.8 nm, and the slit width was 0.5 nm. The lamp current was 4.0 mA in both cases.

X-ray diffraction (XRD) was carried out to identify the crystal structure and crystallite size of the clay. The XRD patterns were recorded in the 2θ range of 5°–50° in a (Shimadzu X-600, Japan) powder diffractometer with CuKα1 radiation for structural analysis operated at 40 kV. Surface area measurements were performed using the surface analyzer.

X-ray fluorescence (XRF) analysis was performed on the ZSX Primus II (Rigaku, USA) to determine the metals content in clay samples as metal oxides. Clay samples were heated to 900°C for 8 h to convert all metals to metal oxides to avoid interaction with the platinum crucible. XRF sample was then prepared according to fusion procedure by mixing 0.3 g of the obtained metal oxides from the sample with 6.7 g of lithium borates flux (SPEX, USA). The mixture was then melted at 1,100°C using an automatic fusion system (Katanax, Canada) to make a glass disk in a platinum fusion disk mold. The elemental composition of each sample was finally analyzed using an XRF spectrometer (Rigaku, USA).

The functionality of the natural clay particles as well as recycled clay samples after adsorption with different concentrations of Ni and Cd was measured by a Nicolet iS10 attenuated total reflectance-Fourier transform infrared (FTIR) spectrometer in the range of 4,000–400 cm^{-1} at a spectral resolution of 4 cm^{-1}. The morphologies of the natural clay materials before and after adsorption of Ni and Cd ions were performed on benchtop scanning electron microscope (TM3030Plus SEM, Hitachi). Moreover, the elemental compositions and locations of different elements were obtained on SEM equipped with an energy dispersive X-ray (EDX, Oxford Instrument, Oxfordshire, UK) spectrometer.

The BET surface area analysis, pore size and pore volume of natural clay before and after adsorption studies were analyzed according to the multipoint N_2 adsorption–desorption method at 77.3 K using Micromeritics TriStar 3000 surface analyzer (Norcross, US). The clays were degassed in an oven at 120°C under a vacuum of 10 mm Hg for 24 h to remove any moisture and/or absorbed contaminant gases on the surface of the clay particles before analysis. The N_2 adsorption isotherms (five points of relative pressure P/P_0 between 0.05 and 0.2) were used to calculate the BET surface area while the desorption isotherms were used to obtain the average pore size and total pore volume using the BJH method.

2.4. Langmuir and Freundlich isotherms

The Langmuir isotherm assumes adsorption of a monolayer on a uniform surface with a specific quantity of adsorption sites. Once a site is occupied, no lateral interactions between the sorbed molecules take place at that site [48]. The Langmuir isotherm pattern is represented by Eq. (3):

$$\frac{C_e}{q_e}=\frac{1}{bq_m}+\frac{C_e}{q_m} \tag{3}$$

where q_m refers to maximum adsorption capacity (mg/g), and b refers to the Langmuir constant associated with the adsorption speed.

The separation factor, b, shown in Eq. (4) is used to realize the attraction strength between the clay and adsorbed metal.

$$R_L = \frac{1}{1 + bC_0} \tag{4}$$

Here, the R_L value gives essential information about the nature of adsorption.

The Freundlich isotherm model was applied to adsorption on multilayer heterogeneous surfaces with the interaction between adsorbed molecules [49]. The Freundlich isotherm is an empirical equation (Eq. (5)) that could be used to define heterogeneous systems.

$$\log q_e = \log k_f + \frac{1}{n}\log C_e \tag{5}$$

where k_f refers to adsorption capacity of sorbent and the value of n determines the degree of non-linearity between solution concentration and adsorption in the following manner: if $n = 1$, then adsorption would be linear; if $n > 1$, then adsorption would be a chemical process and if $n < 1$, then adsorption would be a physical process.

3. Results and discussion

3.1. Characterization of natural clay

The particle size and surface morphology features of the used clay were studied using SEM as shown in Fig. 1. The SEM images showed that the clay sample had mixed morphology, where some larger particles exhibit irregular shape, some particles have an elongated rod-like structure and other smaller particles showing rectangular shape with rough corners. Overall, most of the particles seem to have a thin and rough structure with irregular edges. The clay sample also showed a wide range of particles sizes. The larger particles are in the range of 2–8 μm size, whereas the smaller particles are mostly in the sub-micron size range.

The XRD pattern of the clay sample is shown in Fig. 2. The graph shows many clear, sharp peaks of different intensities, indicating the good crystalline nature of the clay sample. The XRD peaks were matched with the XRD standard database. The highest intensity peak found at 3.22 Å d-spacing corresponds to the feldspar, forming as primary minerals in clay sample studied. Another peak found at 2.04 Å d-spacing was attributed to the presence of illite in clay. Other distinctive peaks found at 2.147, 2.497, and 2.958 Å d-spacing indicate the presence of quartz, calcite and gypsum traces in the sample.

The clay sample was also characterized by BET analysis using N_2 sorption to determine its surface area, pore size and pore volume. Based on the structure of solids under analysis, the adsorption of gases and vapors gives rise to I–VI types of the isotherm. Fig. 3 shows the isotherm for the studied clay sample which exhibits isotherm type IV with H_2-type hysteresis loop [50]. This type of pattern is typical of mesoporous materials which are associated with a capillary condensation in bottle-pore shape. The BET surface area was found to be 35 ± 1 m^2/g and the average pore size 6.5 ± 0.5 nm of clay particles. The total pore volume, for pores with a diameter less than 133.08 nm at P/P_0 = 0.9854, was 5.690e-02 cc/g. This confirms that the clay sample exhibit a mesoporous structure as expected. The mesopore is present throughout the whole sample and form a highly interpenetrating and uniform porous network. These results are in close agreement with another published study on local

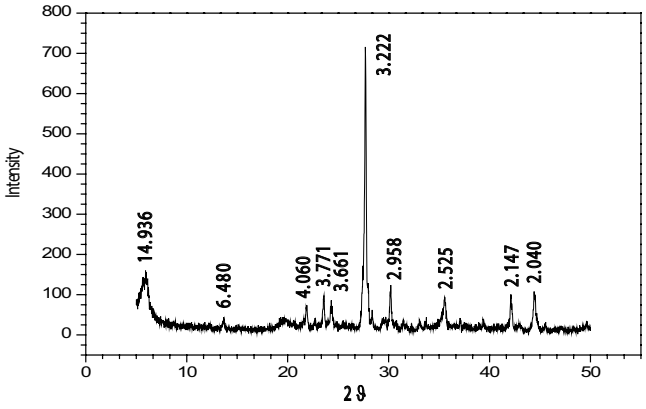

Fig. 2. XRD pattern of the clay sample.

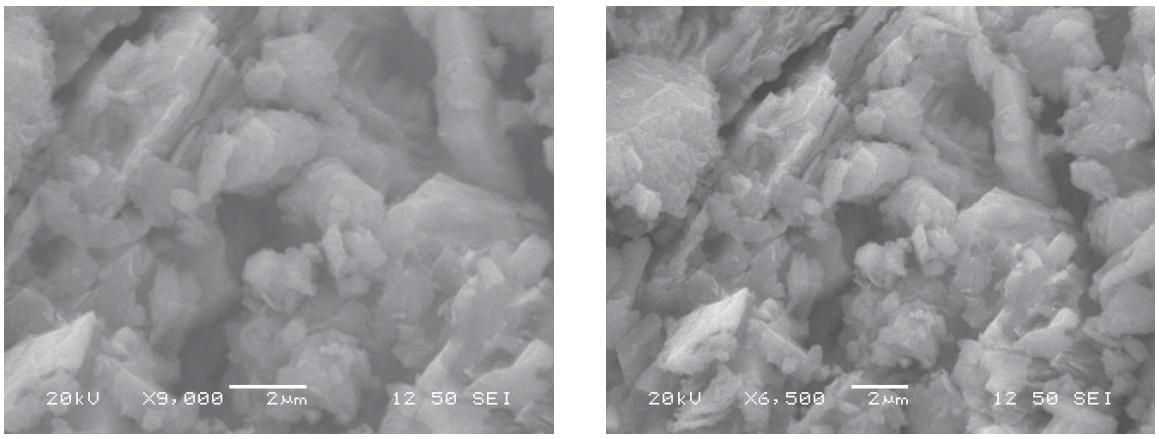

Fig. 1. SEM images of the natural clay sample showing the particle size and morphological features.

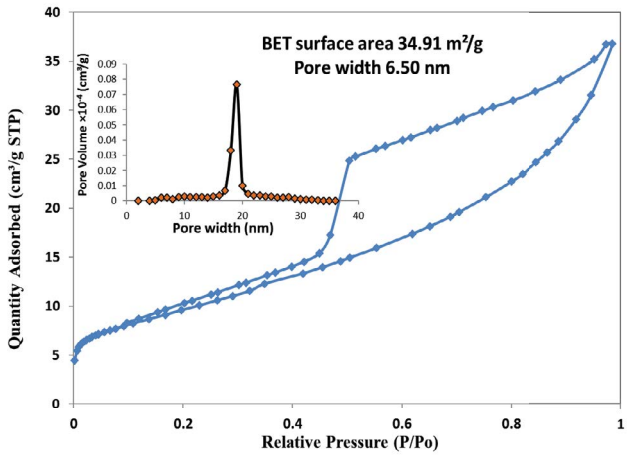

Fig. 3. N_2 adsorption–desorption isotherm of natural clay sample (inset shows the pore size distribution).

bentonite clay from Jeddah, Saudi Arabia [4]. The clay was characterized and tested for its ability to adsorb Cu and Ni from wastewater. The BET surface area was reported to be 62.57 m^2/g, pore volume (P/P_0 = 0.97) of 0.098 cm^3/g, and average pore width of 62.7 Å.

Table 2 summarizes the XRF analysis for clay sample. It was found that the clay sample contained highest amount of SiO_2 (47.33%) while the other major components were Al_2O_3 and Fe_2O_3 with 18.14% and 15.89%, respectively. CaO and MgO were also present in amounts of 7.74% and 5.08%, respectively. Few other materials such as TiO_2 and K_2O were also present in trace amounts. The chemical composition of this clay closely matched with another reported clay from Jeddah, Saudi Arabia [4,30]. The main matched compounds reported were also SiO_2 (58%), Al_2O_3 (20%) and Fe_2O_3 (5.17%) with others such as TiO_2, MgO, CaO and K_2O in minor quantities. The chemical composition is also similar to Khulays activated clay (bentonite) from Jeddah, Saudi Arabia, used to remove Ni from wastewater [31].

Table 2
XRF analysis of the clay sample

Metal oxides	Elemental chemical composition wt.%
SiO_2	47.33
Fe_2O_3	15.89
Al_2O_3	18.14
TiO_2	1.67
CaO	7.74
K_2O	0.63
MgO	5.08

3.2. Effect of clay dosage

The effect of clay dosage on Ni and Cd metals removal efficiency from aqueous solutions are shown in Fig. 4. At 0.4 g clay, Ni removal was observed to be around 94% while Cd residue was out of the AAS range for the same clay amount and only effective at 0.6 g clay for Cd. In both cases, the metal removal efficiency increased with increasing clay dosage up to 1.2 g (Fig. 4). With clay loading between

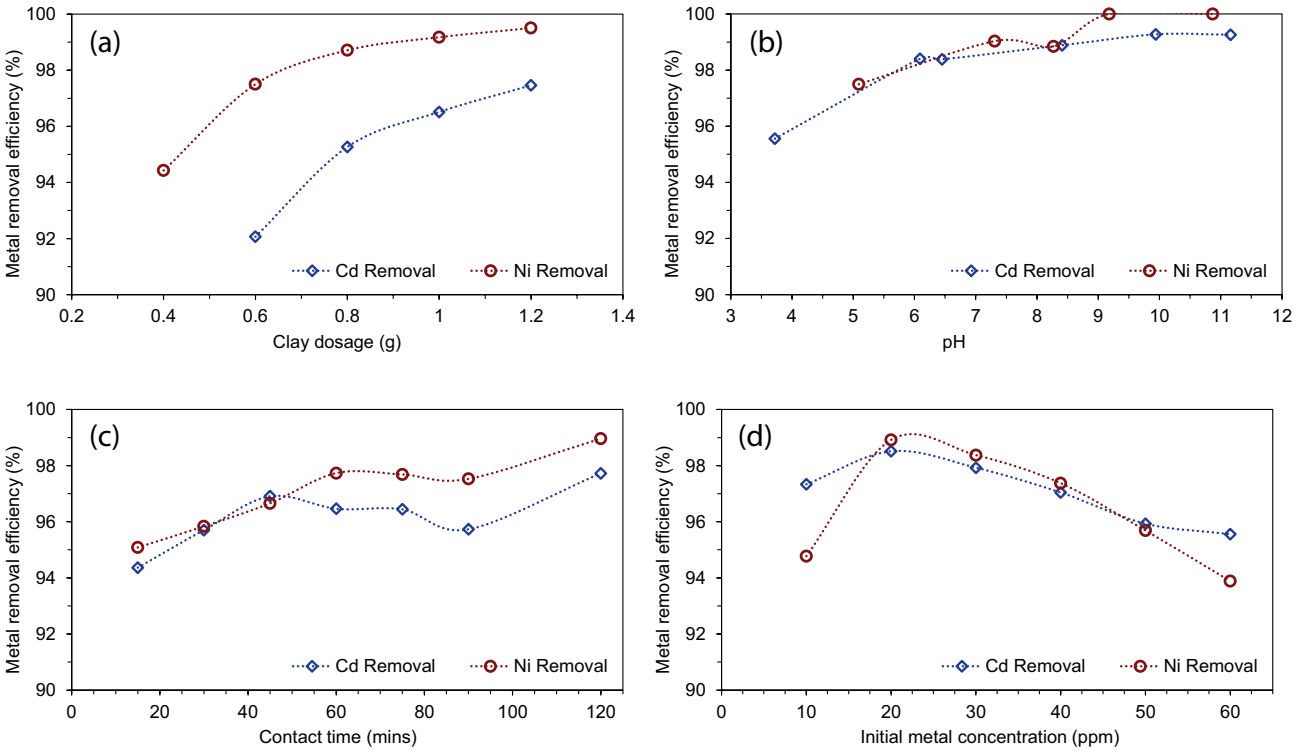

Fig. 4. (a) Effect of clay dosage, (b) pH, (c) contact time, and (d) initial metal ions concentration on metals removal efficiency.

1–1.2 g, the removal efficiency curves of both metals seem to flatten indicating that the 1.2 g clay may be considered as the optimum dosage with maximum efficiencies of 99.5% for Ni and 97.5% for Cd. Overall, the clay showed higher removal efficiency for Ni than Cd for all studied clay dosage values.

3.3. Effect of pH and contact time

The Ni and Cd metal ion solutions were prepared with concentrations of 40 ppm and pH in the range of 4–11. The metal removal efficiencies of both metals were higher in alkaline solutions than acidic solutions studied (Fig. 4). It may be concluded that although higher removal efficiencies were observed at pH values greater than 7, the clay is capable of removing almost 98% of the heavy metals even at around neutral pH. As the pH of the solution increases, the % removal efficiency also increases. This observation is in a good agreement with the behavior observed by Al-Shihrani [31–33]. This behavior was anticipated because adsorption of heavy metal ions onto clay is significantly affected by the pH of the solution. According to various researchers, three distinct regions are observed in the heavy metal ions adsorption vs. pH graphs. Usually, region 1 is low pH region (pH range 1–4), where up to 40% of Cd ions are reported to get adsorbed followed by region 2 (pH range 4–6) where up to 90% of the Cd ions get adsorbed. The third region (6–12), where more than 90% of Cd ions removal is observed. However, in the current work, the minimum pH range starts from around 4 and the Cd ions removal is already more than 90% which agrees with Kostin et al. [51]. The pH range in the current work begins with removal efficiencies higher than 90% at pH higher than 4. Thus, it may be assumed that since deprotonation of the mineral surface takes place at higher pH values, the clay might become negatively charged leading to electrostatic attraction between the positively charged metal ions and the negatively charged clay mineral surfaces as reported by Kostin et al. [51]. This clay is economically favorable as higher removal efficiencies can be achieved without any need for expensive pH control and adjustment.

The effect of contact time on metal removal efficiency was investigated using the optimum clay dosage of 1.2 g and neutral aqueous solutions. The samples of both Ni and Cd metals were prepared using 40 ppm contamination in 50 mL aqueous solutions. Overall the increasing metal removal efficiency was observed with increase in contact time for both systems. The removal efficiency of almost 94% was observed just after 15 min of contact time, suggesting that the active sites on the clay surface have reached close to saturation point. As the contact time increased from 15 min up to 120 min, the metal removal efficiency increased up to around 98%. However, around 97% efficiency was obtained within a short time of 60–75 min of mixing as shown in Fig. 4, which is favorable for process economic reasons. Nevertheless, depending on the environmental legislation and health regulations, 97% removal efficiencies of these metal ions after just 1 h of mixing may be sufficient and acceptable.

3.4. Effect of initial metal ions concentration

The effect of initial metal ions concentration on removal efficiency was investigated using the obtained optimum conditions. The Ni and Cd aqueous solutions of 10, 20, 30, 40, 50 and 60 ppm were prepared and tested for metal adsorption on clay particles of 1.2 g quantities. The trends of metal removal efficiency were similar for both systems. The metal removal efficiencies decreased as the initial metal ion concentrations increased. The removal efficiencies were

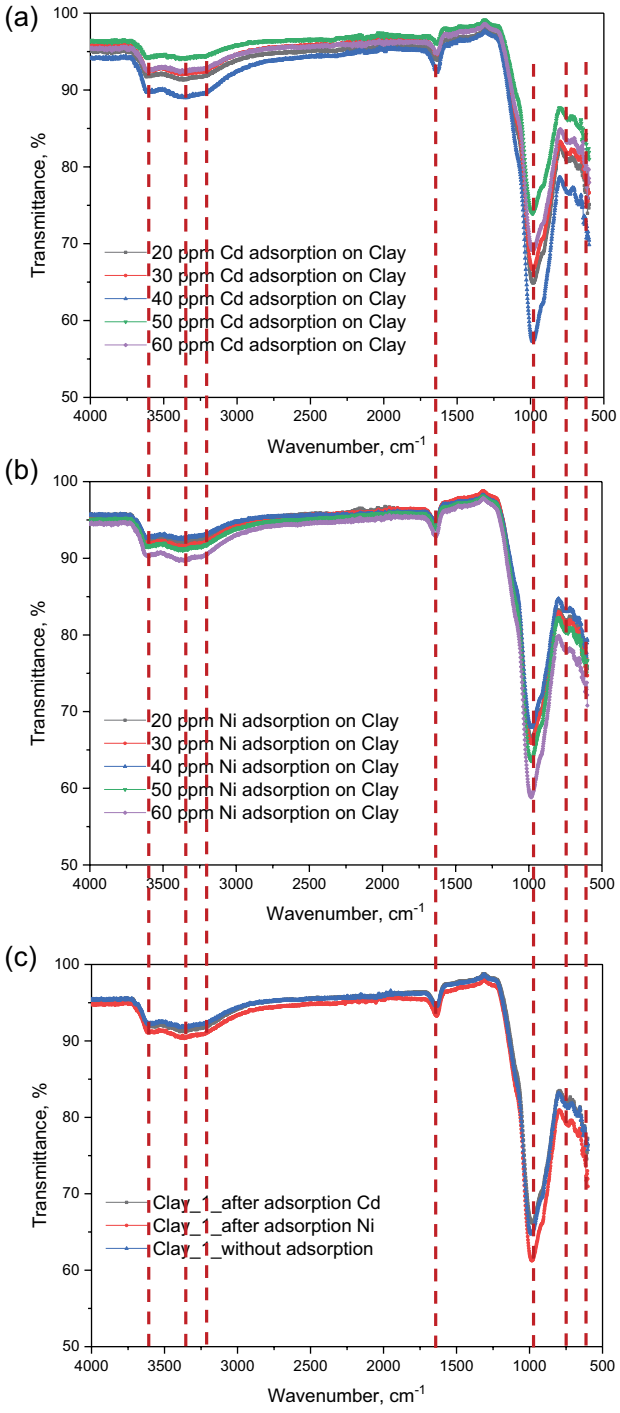

Fig. 5. FTIR spectra for clay samples (a) after different concentration of Cd ions adsorptions, (b) after different concentrations of Ni ions adsorptions, and (c) clay particles with and without Ni and Cd ions adsorptions.

found in decreasing range of 98%–94% for the concentration range between 10 and 60 ppm as shown in Fig. 4.

3.5. Characterization of natural clay before and after metal adsorption studies

FTIR spectra for clay particles with and without adsorption of Ni and Cd ions are presented in Fig. 5. It can be seen that there are three main set of peaks for all samples in the range of 600–1,200; 1,575–1,700; and 2,800–3,740 cm^{-1}. The board peak at 3,355 cm^{-1} corresponds to the multilayer water molecules in clay samples with and without adsorptions of Ni and Cd ions. This is also accompanied by a well-defined shoulder peak at 3,250 cm^{-1} which is possibly related to the free water molecules (bound water) on the surface of clay molecule structure. The peaks appearance at 3,585 and 3,600 cm^{-1} can be assigned to the Al–O–H (inter-octahedral) and Al–O–H stretching, respectively [52]. The observed weak peak at 1,640 cm^{-1} is attributed to the bending of water molecules (H–O–H). There are several peaks appeared at 1,115 and 985 cm^{-1} due to Si–O stretching while the bending of Al–Al–OH bonds is present at 915 cm^{-1}. Some weak peaks can be observed in the range of 600–780 cm^{-1} due to Si–O–Al bending, Si–O Stretching, Si–O–Si bending and Si–O bonds [52,53]. Nevertheless, there is no significant change in the FTIR peaks position or new peaks emerged due to the adsorption of metals ions as expected.

The elemental compositions and mapping of different elements in natural clay sample before and after adsorption of Cd and Ni ions were studied on SEM/ EDX (Fig. 6). These images show a nice distribution of different elements in different colors with some indication of their concentrations. The common elements found in all natural clay samples before and after adsorption are O, Si, Na, Al, Ca, Ti, Fe, Mg, K. The Cd element represented by green color can be clearly seen from the natural clay used for the adsorption of Cd ions (Fig. 6b). Similarly, Ni element is also shown in red color from the clay sample after Ni adsorption study (Fig. 6c). This further proves that the Cd and Ni ions were successfully adsorbed onto the natural clay material. It is interesting to note that both mapping images show abundant and even distribution of Cd or Ni elements that further confirms natural clay is a good material for adsorption of metal ions.

The BET surface area, average pore size, and total pore volume were analyzed for the natural clay sample before and after adsorption with Cd and Ni ions as a comparative study (Fig. 7). Table 3 shows the data for a range, 20–60 ppm, of Cd and Ni adsorbed clay samples as well as natural clay without adsorption. The BET surface area of 25.16 m^2/g and the average pore size and pore volume of 5.02 nm and 3.9e-02 cm^3/g, respectively, were obtained for natural clay without adsorption. Overall, the adsorption of metal ions reduced the BET surface area, pore size and volume as expected. For example, the clay sample after adsorption of 60 ppm Cd showed a surface area of 17.14 m^2/g, the pore size of 4.67 nm and pore volume of 3.1e-02 cm^3/g. These results are in agreement with SEM/EDX data and further confirm that the metal ions were

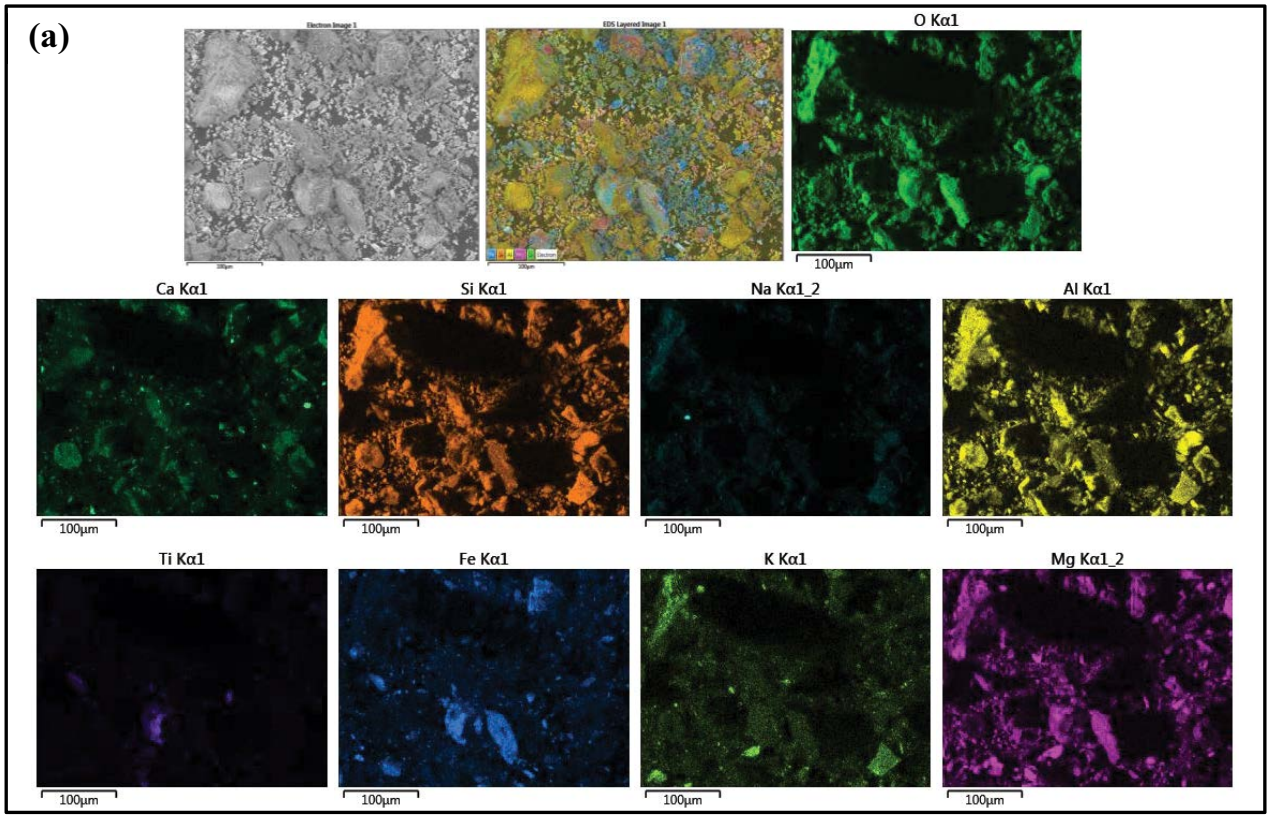

(Fig. 6. Continued)

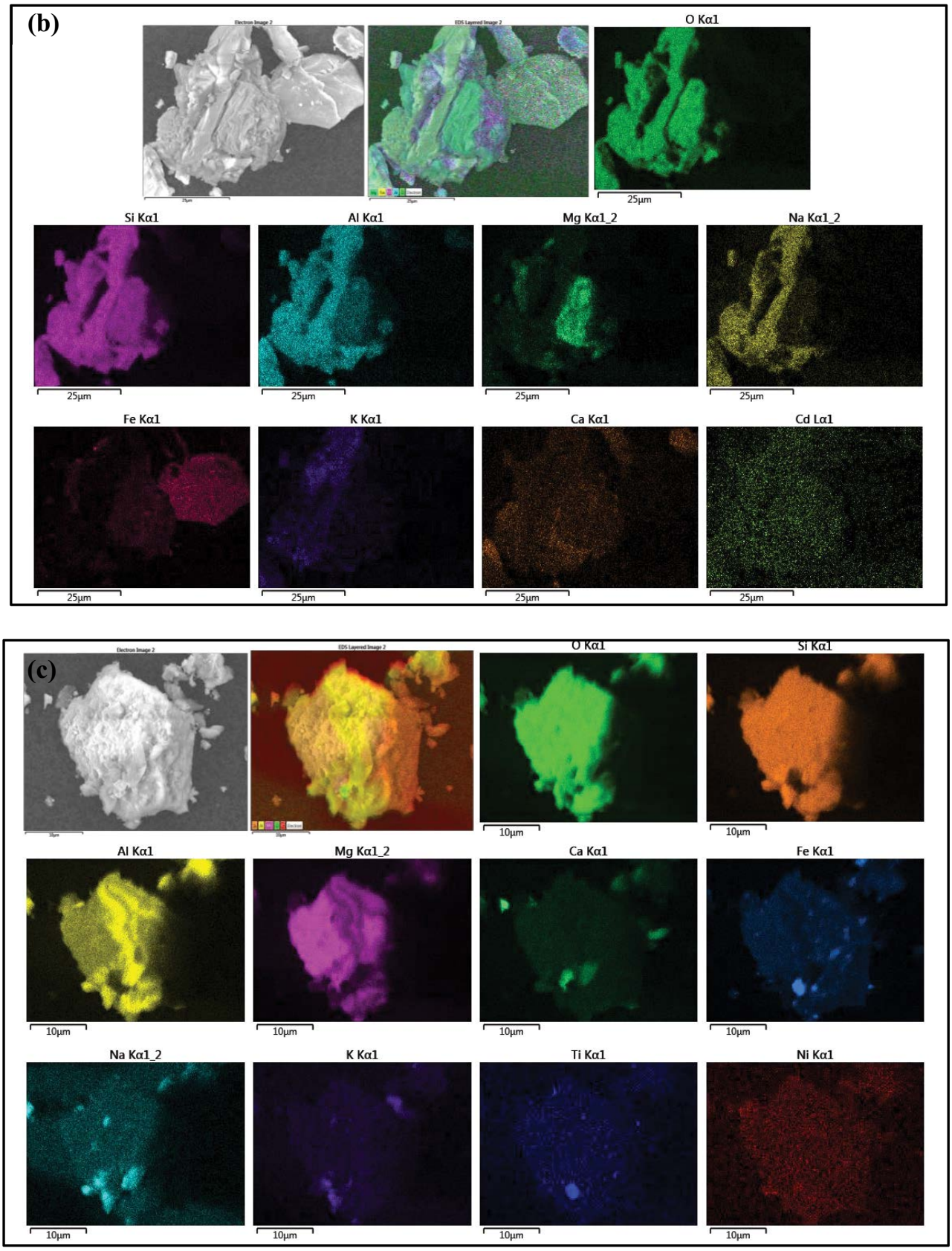

Fig. 6. SEM/EDX analysis showing the elemental composition of (a) natural clay before adsorption of metal ions, (b) natural clay after adsorption of Cd ions, and (c) natural clay after adsorption of Ni ions.

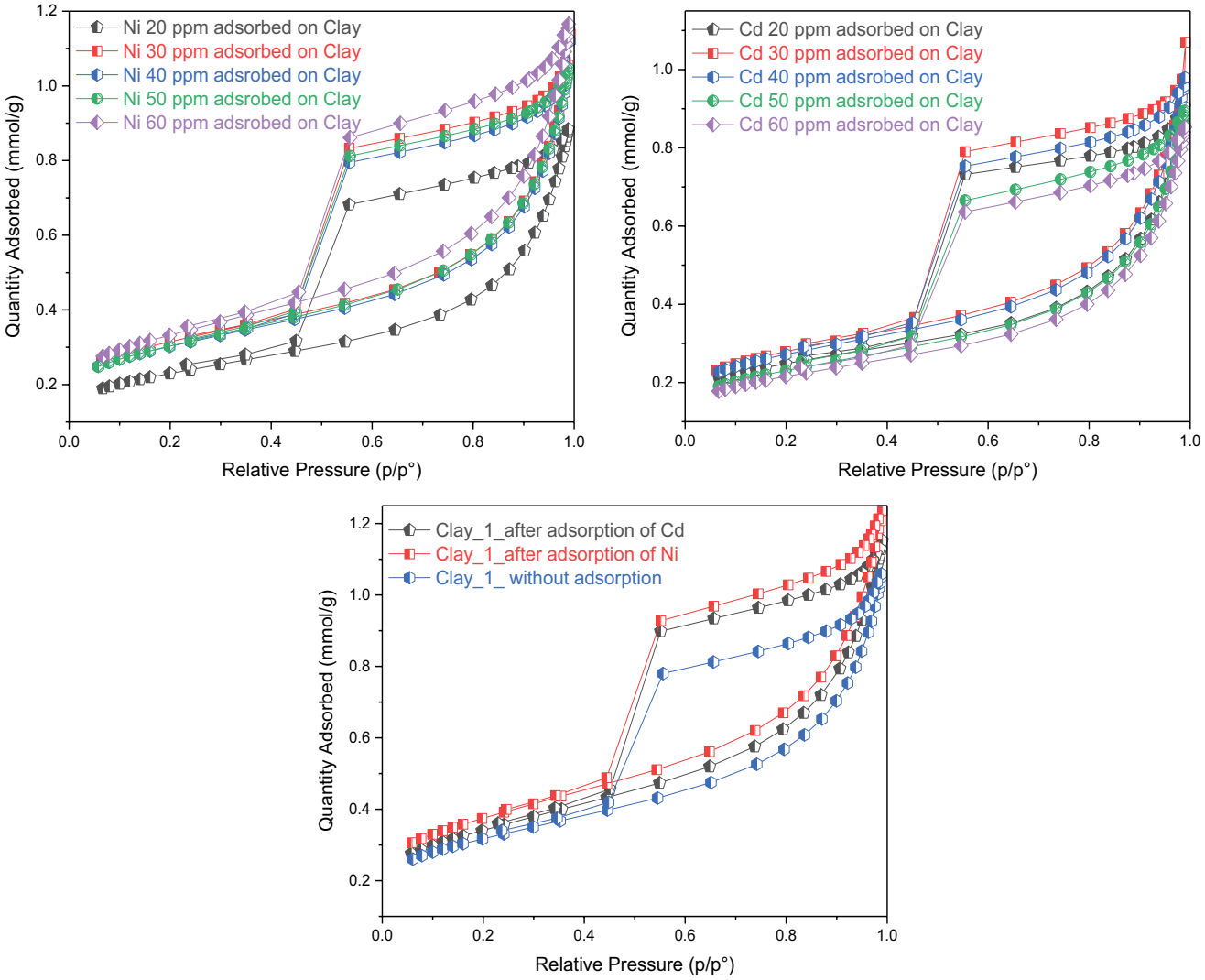

Fig. 7. N_2 porosimetry curves of natural clay before and after adsorptions of Ni and Cd.

Table 3
BET surface areas, external BET surface area, BJH average pore diameter and total pore volume for all samples

Sample code label	BET method	BJH method	
	Surface area ($m^2 g^{-1}$)	Total pore volume ($cm^3 g^{-1}$)	Average pore size (nm)
20 ppm Cd adsorbed on clay	19.62 ± 0.17	0.033	4.345
30 ppm Cd adsorbed on clay	22.09 ± 0.18	0.039	4.87
40 ppm Cd adsorbed on clay	21.50 ± 0.18	0.035	4.66
50 ppm Cd adsorbed on clay	18.32 ± 0.19	0.032	4.72
60 ppm Cd adsorbed on clay	17.14 ± 0.11	0.031	4.67
20 ppm Ni adsorbed on clay	18.24 ± 0.12	0.032	4.53
30 ppm Ni adsorbed on clay	24.84 ± 0.20	0.041	4.92
40 ppm Ni adsorbed on clay	23.92 ± 0.18	0.040	5.07
50 ppm Ni adsorbed on clay	24.03 ± 0.16	0.038	4.64
60 ppm Ni adsorbed on clay	26.37 ± 0.16	0.042	4.93
Natural clay without adsorption of metals	25.16 ± 0.16	0.039	5.02

adsorbed onto the natural clay, resulting in the overall reduction of BET surface area, pore size and volume. Note that the new values are slightly lower than the first set of data for only natural clay sample without adsorption as given above. However, this difference is within allowable surface area measurement errors.

3.6. Experimental data fitted into Langmuir and Freundlich isotherm models

The experimental data found in this study were fitted into the Langmuir isotherm model to estimate the maximum adsorption capacity of Saudi natural clay for Ni and Cd metals. Linear plots of C_e/q_e vs. C_e (Fig. 8) indicate the applicability of the Langmuir isotherm model. Values of q_m and b were determined graphically from the gradients and intercepts, respectively, and are shown in Table 4. The Langmuir isotherm is classified as an irreversible process when $R_L = 0$, a favorable process when $0 < R_L < 1$, linear process when $R_L = 1$, or unfavorable process when $R_L > 1$. The R_L values for all initial concentrations were found in between 0 and 1 (Table 4), which indicate that adsorption of both Ni and Cd ions on the natural clay was a favorable process.

The experimental data were also fitted into the Freundlich isotherm model. The graphs constructed for ln q_e against ln C_e showed a linear trend (Fig. 9) that indicates the applicability of the Freundlich model. The adsorption capacity (K_f) can be estimated from intercept and adsorption intensity (n) from the slope of this graph. As shown in Table 4, the n value for Cd(II) > 1 indicating favorable adsorption. However, the n value for Ni(II) is < 1 that indicates unfavorable adsorption on the natural clay investigated which is also confirmed by the low value of adsorption capacity. The maximum adsorption capacity (q_m) for Cd ions removal was 3.31 mg/g clay calculated from the Langmuir isotherms. This is in good agreement with the work of Bedoui et al. [54] who used pure smectite and reported a maximum adsorption capacity of 3.87 mg/g clay. As for the Ni ions removal, a q_m value of 2.7 mg/g clay was observed in this study, which is similar to the 7.1 mg/g reported by Gupta and Bhattacharyya [55] for kaolinite and 2.236 mg/g for sepiolite [56]. For the adsorption of metal ions onto clay, two possible mechanisms are reported in the literature which includes the ion exchange and the formation of complexes with hydroxyl groups on the clay surface. In the low pH range, the ion exchange process predominates while the formation of complexes usually occurs in the higher pH range [51].

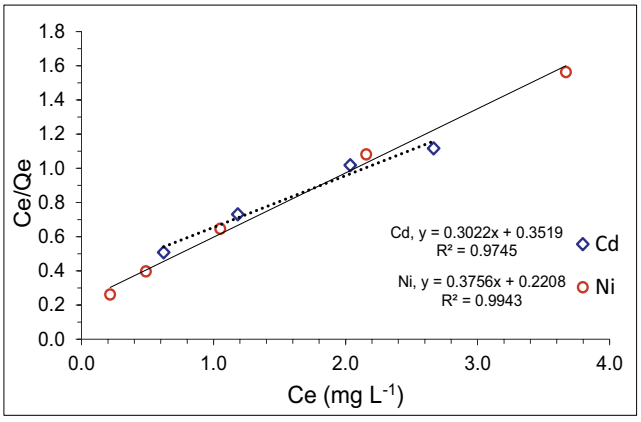

Fig. 8. Langmuir isotherm models for both metals.

Table 4
Isotherm studies for the adsorption of Cd(II) and Ni(II) ions onto natural clay

	Ni(II)	Cd(II)
	Langmuir isotherm	
q_m	2.7 mg/g clay	3.3 mg/g clay
b	1.7	0.86
R_L	0.056, 0.029, 0.019, 0.014, 0.012, and 0.010	0.104, 0.055, 0.037, 0.028, 0.023, and 0.019
R^2	0.99	0.97
	Frenudlich isotherm	
n	0.37	2.23
K_f	0.61	1.2
R^2	0.98	0.99

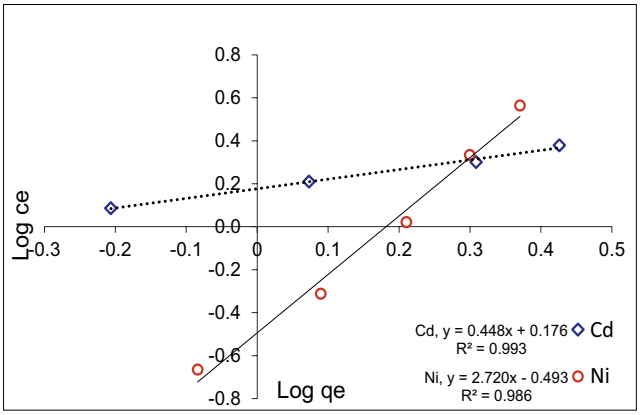

Fig. 9. Freundlich isotherm model for both metals.

4. Conclusions

In this work, Saudi natural clay has been utilized as an efficient (removal efficiency of above 90%), cheap, environment-friendly and natural adsorbent material for the removal of Cd and Ni metal ions from artificial wastewater. The clay retained substantial amounts of both metals, Cd, and Ni readily, but it showed a higher affinity for the Cd metal ions. This clay inherently possesses certain characteristics that make it suitable for wastewater treatment. These include: (1) economy – this material is very cheap. The only cost of this material would be for the extraction, transportation, crushing, and grinding. It does not require any modification or alteration, (2) availability – this material is abundantly available in the region, (3) effectiveness – it is capable of removing Cd as well as Ni. This clay might be suitable for removing other heavy metals and pollutants that require further research.

Acknowledgments

The authors extend their appreciation to the Deanship of Scientific Research at King Khalid University for funding this work through research groups program under grant number R.G.P1./97/40.

References

[1] Y.A. Aggour, M. Diab, T. Hegazy, S.E. Halawia, Removal of cadmium, lead, zinc, copper and iron from their aqueous solution by kaolinite clay, Int. J. Adv. Res., 3 (2015) 1922–1934.
[2] S.A.M.A.S. Eqani, R. Khalid, N. Bostan, Z. Saqib, J. Mohmand, M. Rehan, N. Ali, I.A. Katsoyiannis, H. Shen, Human lead (Pb) exposure via dust from different land use settings of Pakistan: a case study from two urban mountainous cities, Chemosphere, 155 (2016) 259–265.
[3] N. Rahmanian, S.H.B. Ali, M. Homayoonfard, N.J. Ali, M. Rehan, Y. Sadef, A.S. Nizami, Analysis of Physiochemical Parameters to Evaluate the Drinking Water Quality in the State of Perak, Malaysia, J. Chem., 2015 (2015) 1–10.
[4] S.A. Aljlil, F.D. Alsewailem, Adsorption of Cu and Ni on bentonite clay from waste water, Athens J. Sci., 1 (2014) 21–30.
[5] FAO: Food and Agriculture Organization of the United Nations, Water Quality for Irrigation and Drainage, Paper No. 10. FAO, Rome, 1985.
[6] M. Arshadi, M.J. Amiri, S. Mousavi, Kinetic, equilibrium and thermodynamic investigations of Ni(II), Cd(II), Cu(II) and Co(II) adsorption on barley straw ash, Water Resour. Ind., 6 (2014) 1–17.
[7] Z. Abbasi, M. Alikarami, E.R. Nezhad, F. Moradi, V. Moradi, Adsorptive removal of Co^{2+} and Ni^{2+} by peels of banana from aqueous solution, Universal J. Chem., 1 (2013) 90–95.
[8] G. Sharma, A. Kumar, M. Naushad, A. Kumar, A.H. Al-Muhtaseb, P. Dhiman, A.A. Ghfar, F.J. Stadler, M.R. Khan, Photoremediation of toxic dye from aqueous environment using monometallic and bimetallic quantum dots based nanocomposites. J. Cleaner Prod., 172 (2018) 2919–2930.
[9] A. Kumar, M. Naushad, A. Rana, G. Sharma, A.A. Ghfar, F.J. Stadler, M.R. Khan, ZnSe-WO_3 nano-hetero-assembly stacked on Gum ghatti for photo-degradative removal of Bisphenol A: symbiose of adsorption and photocatalysis, Int. J. Biol. Macromol., 104 (2017) 1172–1184.
[10] G. Sharma, D. Pathania, M. Naushad, Preparation, characterization and antimicrobial activity of biopolymer based nanocomposite ion exchanger pectin zirconium (IV) selenotungstophosphate: application for removal of toxic metals, J. Ind. Eng. Chem., 20 (2014) 4482–4490.
[11] M. M. Barbooti, Simultaneous removal of chromium and lead from water by sorption on Iraqi montmorillonite, J. Environ. Prot., 6 (2015) 237–249.
[12] Y. Bulut, T. Zek, Adsorption studies on ground shells of hazelnut and almond, J. Hazard. Mater., 149 (2007) 35–41.
[13] Y. Bulut, T. Zek, Removal of heavy metals from aqueous solution by sawdust adsorption, J. Environ. Sci., 19 (2007) 160–166.
[14] M.R. Awual, M.M. Hasan, G.E. Eldesoky, M.A. Khaleque, M.M. Rahman, M. Naushad, Facile mercury detection and removal from aqueous media involving ligand impregnated conjugate nanomaterials, Chem. Eng. J., 290 (2016) 243–251.
[15] M. Naushad, Z.A. Al-Othman, M. Islam, Adsorption of cadmium ion using a new composite cation-exchanger polyaniline Sn (IV) silicate: kinetics, thermodynamic and isotherm studies, Int. J. Environ. Sci. Technol., 10 (2013) 567–578.
[16] A.A. Alqadami, M. Naushad, Z.A. Alothman, A.A. Ghfar, Novel metal–organic framework (MOF) based composite material for the sequestration of U (VI) and Th (IV) metal ions from aqueous environment, ACS Appl. Mate. Interfaces, 9 (2017) 36026–36037.
[17] M. Naushad, T. Ahamad, B.M. Al-Maswari, A.A. Alqadami, S.M. Alshehri, Nickel ferrite bearing nitrogen-doped mesoporous carbon as efficient adsorbent for the removal of highly toxic metal ion from aqueous medium, Chem. Eng. J., 330 (2017) 1351–1360.
[18] R. Bushra, M. Naushad, R. Adnan, Z.A. ALOthman, M. Rafatullah, Polyaniline supported nanocomposite cation exchanger: synthesis, characterization and applications for the efficient removal of Pb^{2+} ion from aqueous medium, J. Ind. Eng. Chem., 21 (2015) 1112–1118.
[19] A.A. Alqadami, M. Naushad, M.A. Abdalla, T. Ahamad, Z.A. ALOthman, S.M. Alshehri, A.A. Ghfar, Efficient removal of toxic metal ions from wastewater using a recyclable nanocomposite: a study of adsorption parameters and interaction mechanism, J. Cleaner Prod., 156 (2017) 426–436.
[20] Y. Gutha, V.S. Munagapati, M. Naushad, K. Abburi, Removal of Ni (II) from aqueous solution by *Lycopersicum esculentum* (Tomato) leaf powder as a low-cost biosorbent, Desal. Wat. Treat., 54 (2015) 200–208.
[21] M. El-Sadaawy, O. Abdelwahab, Adsorptive removal of nickel from aqueous solutions by activated carbons from doum seed (*Hyphaenethebaica*) coat, Alexandria Eng. J., 53 (2014) 399–408.
[22] A. Omri, M. Benzina, Removal of manganese (II) ions from aqueous solutions by adsorption on activated carbon derived a new precursor: *Ziziphus spina-christi* seeds, Alexandria Eng. J., 51 (2012) 343–350.
[23] M.A.O. Badmus, T.O.K. Audu, B.U. Anayata, Removal of lead ion from industrial wastewaters by activated carbon prepared from periwinkle shells (*Typanotonus fuscatus*), Turkish J. Eng. Env. Sci., 31 (2007) 251–263.
[24] P.S. Kumar, Adsorption of lead (II) ions from simulated wastewater using natural waste: a kinetic, thermodynamic and equilibrium study, Environ. Prog. Sustain. Energy, 33 (2014) 55–64.
[25] G. Moussavi, R. Khosravi, Removal of cyanide from wastewater by adsorption onto pistachio hull wastes: parametric experiments, kinetics and equilibrium analysis, J. Hazard. Mater., 183 (2010) 724–730.
[26] N. Rajamohan, M. Rajasimman, R. Rajeshkannan, V. Saravanan, Equilibrium, kinetic and thermodynamic studies on the removal of Aluminum by modified *Eucalyptus camaldulensis* barks, Alexandria Eng. J., 53 (2014) 409–415.
[27] G. Sharma, M. Naushad, A. Kumar, S. Rana, S. Sharma, A. Bhatnagar, F.J. Stadler, A.A. Ghfar, M.R. Khan, Efficient removal of coomassie brilliant blue R-250 dye using starch/poly (alginic acid-cl-acrylamide) nanohydrogel, Process Saf. Environ. Prot., 109 (2017) 301–310.
[28] R. Bushra, M. Naushad, G. Sharma, A. Azam, Z.A. ALOthman, Synthesis of polyaniline based composite material and its analytical applications for the removal of highly toxic Hg^{2+} metal ion: Antibacterial activity against *E. coli*, Korean J. Chem. Eng., 34 (2017) 1970–1979.
[29] G. Sharma, M. Naushad, D. Pathania, A. Kumar, A multifunctional nanocomposite pectin thorium (IV) tungstomolybdate for heavy metal separation and photoremediation of malachite green, Desal. Wat. Treat., 57 (2016) 19443–19455.
[30] S.A. Aljlil, F.D. Alsewailem, Saudi Arabian clays for lead removal in wastewater, Appl. Clay Sci., 42 (2009) 671–674.
[31] S.S. Al-Shahrani, Treatment of wastewater contaminated with nickel using khulays activated bentonite, Int. J. Eng. Technol. IJET-IJENS, 12 (2012).
[32] S.S. Al-Shahrani, Removal of cadmium from waste water using Saudi activated bentonite, WIT Trans. Ecol. Environ., 163 (2012) 391–402.
[33] S.S. Al-Shahrani, Treatment of wastewater contaminated with cobalt using Saudi activated bentonite. Alexandria Eng. J., 53 (2014) 205–211.
[34] N. Zahra, Adsorption of Lead from wastewater on Pakistani bentonites, Am. J. Sci. Ind. Res., 3 (2012) 387–389.
[35] Ö. Yavuz, Y. Altunkaynak, F. Guzel, Removal of copper, nickel, cobalt and manganese from aqueous solution by kaolinite, Water Res., 37 (2003) 948–952.
[36] Ö. Yavuz, R. Guzel, F. Aydin, I. Tegin, R. Ziyadanogullari, Removal of cadmium and lead from aqueous solution by calcite, Polish J. Environ. Stud., 16 (2007) 467–471.

[37] J.S. Essomba, J. Ndi Nsami, P.D. Bilibi Bilibi, G.M. Tange, J. Ketcha Mbadcam, Adsorption of Cd (II) ions from aqueous solution onto kaolinite and metakaolinite, Pure Appl. Chem. Sci., 2 (2014) 11–30.
[38] J.M. Zachara, C.E. Cowan, C.T. Resch, Sorption of divalent metals on calcite, Geochimica et Cosmochimica Acta, 55 (1991) 1549–1562.
[39] A.T. Sdiri, T. Higashi, F. Jamoussi, Adsorption of copper and zinc onto natural clay in single and binary systems, Int. J. Environ. Sci. Technol., 11 (2014) 1081–1092.
[40] Z. Mohamed, A. Abdelkarim, K. Ziat, S. Mohamed, Adsorption of Cu(II) onto natural clay: Equilibrium and thermodynamic studies, J. Mater. Environ. Sci., 7 (2016) 566–570.
[41] C.A. Christophi, L. Axe, Competition of Cd, Cu and Pb adsorption on goethite, J. Environ. Eng., 126 (2000) 66–74.
[42] W.A. Carvalho, C. Vigando, J. Fontana, Ni(II) removal from aqueous effluents by silylated clays, J. Hazard. Mater., 153 (2008) 1240–1247.
[43] Z. Hongxia, W. Xiaoyun, L. Honghong, T. Tianshe, W. Wangsuo, Adsorption behaviour of Th(IV) onto illite: effect of contact time, pH value, ionic strength, humic acid and temperature, Appl. Clay Sci., 127 (2016) 35–43.
[44] M. Torab-Mostaedi, H. Ghassabzadeh, M. Ghannadi-Maragheh, S.J. Ahmadi, H. Taheri, Removal of cadmium and nickel from aqueous solution using expanded perlite, Brazilian J. Chem. Eng., 27 (2010) 299–308.
[45] M. Eloussaief, I. Jarraya, M. Benzina, Adsorption of copper ions on two clays from Tunisia: pH and temperature effects, Appl. Clay Sci., 46 (2009) 409–413.
[46] P.N.M. Vasconcelos, W.S. Lima, M.L.P. Silva, A.L.F. Brito, H.M. Laborde, M.G.F. Rodrigues, Adsorption of zinc from aqueous solutions using modified Brazilian grey clay, Am. J. Anal. Chem., 4 (2013) 510–519.
[47] I. Ghorbel-Abid, M. Trabelsi-Ayadi, Competitive adsorption of heavy metals on local landfill clay, Arabian J. Chem., 8 (2015) 25–31.
[48] I. Langmuir, The adsorption of gases on plane surfaces of glass, mica and platinum, J. Am. Chem. Soc., 40 (1918) 1361–1403.
[49] P. Klobes, K. Meyer, R.G. Munro, Porosity and Specific Surface Area Measurements for Solid Materials, U.S. Government Printing Office, Washington, 2006.
[50] H.M.F. Freundlich, Over the adsorption in solution, J. Phys. Chem., 57 (1906) 1100–1107.
[51] A.V. Kostin, L.V. Mostalygina, O.I. Bukhtoyarov, The mechanism of adsorption of zinc and cadmium ions onto bentonite clay, Prot. Met. Phys. Chem. Surfaces, 51 (2015) 477–482.
[52] P.S. Nayak, B.K. Singh, Instrumental characterization of clay by XRF, XRD and FTIR, Bull. Mater. Sci., 30 (2007) 235–238.
[53] M.M. Islam, M.N. Khan, S. Biswas, T.R. Choudhury, P. Haque, T.U. Rashid, M.M. Rahman, Preparation and characterization of bijoypur clay-crystalline cellulose composite for application as an adsorbent, Adv. Mater. Sci., 2 (2017) 1–7.
[54] K. Bedoui, I. Bekri-Abbes, E. Srasra, Removal of cadmium (II) from aqueous solution using pure smectite and Lewatite S 100: the effect of time and metal concentration, Desalination, 223 (2008) 269–273.
[55] S.S. Gupta, K.G. Bhattacharyya, Immobilization of Pb (II), Cd (II) and Ni (II) ions on kaolinite and montmorillonite surfaces from aqueous medium, J. Environ. Manage., 87 (2008) 46–58.
[56] S. Ansanay-Alex, C. Lomenech, C. Hurel, N. Marmier, Adsorption of nickel and arsenic from aqueous solution on natural sepiolite, Int. J. Nanotechnol., 9 (2012) 204–215.